

Form of the Latitude Distribution of Sunspot Activity

V. G. Ivanov*, E. V. Miletskii, and Yu. A. Nagovitsyn

Pulkovo Observatory, Russian Academy of Sciences,
Pulkovskoe shosse 65, St. Petersburg, 196140 Russia

Received March 30, 2011; in final form, April 11, 2011

Abstract—The spatial (latitude) distribution of sunspots is studied, including its dependence on solar activity. It is shown that the latitude distributions of sunspots for a given year can be approximately described by the normal law, with its variance being a linear function of the current level of solar activity. Thus, an increase in activity is accompanied by an expansion of the zone of solar activity, in good agreement with earlier results. As the solar activity increases, the width of the zone of sunspot generation and the latitude maximum of the sunspot density grow somewhat more slowly than the number of sunspots, in agreement with observations. The results obtained can be used to reconstruct the spatial distributions of sunspots in the past, interpret the magnetic activity of stars, and address the requirements of the dynamo theory in the form of constraints imposed on models of cyclicity.

DOI: 10.1134/S1063772911100040

1. INTRODUCTION

To understand cyclic stellar magnetic activity in general and the solar cyclicity in particular, it is important to study the relationships between the total level of activity and the spatial distribution of the activity tracers—active regions and sunspots. Many-year detailed observations on the solar activity enable us to analyze this question for the nearest star.

Several regularities have been discovered for these relationships. The best known is the Spörer law, which describes the relationship between the phase of the 11-year cycle and the mean latitude of sunspots. It was shown by Gleissberg [1], by example of a limited number of cycles, that the width of the spotted zone also depends on the cycle phase [1]. Some other relations have also been found, which are briefly reviewed in [2]. In particular, [2] and the subsequent work [3] report a close relationship between the latitude size of the sunspot zone and the current level of sunspot activity. It was shown that the latitude size of the sunspot zone increases with an increase in activity. However, the latitude distribution of sunspots and its dependence on the activity level remained unclear.

The importance of this question is reflected by the fact that modern theories attribute the distribution of magnetic fields at the solar surface to the nature of their generation in the convective zone. In addition, the quantitative parameters of the observed distributions enable comparative studies of various theoretical models of the 11-year cycle [4]. In particular,

the typical latitude size of the sunspot zone can be compared with the theoretical width of the dynamo wave (see, for example, [5]).

Note that the relationships between the spatial distribution of activity and the sunspot indices are important for the reconstruction of the solar activity over long time intervals. They provide the opportunity to reconstruct both the total level of activity and its spatial distribution [3], including for specific epochs (the Maunder minimum [6], for example), which is very important for the development of realistic dynamo theories [7].

The interpretation of multi-color photometric images of late-type stars [8, 9] used to analyze their cyclic activity is another application of the studies considered here.

The present work examines the latitude distribution of sunspots detected during selected time intervals. This differs from the approach of studying the latitude–time distribution, which usually has the form of the Maunder butterfly diagrams with certain features. In our approach, the choice of the time interval used to calculate the parameters of the latitude distribution is especially important. Earlier studies have used time intervals roughly equal to the period of the 11-year solar cycle [4, 10–12] or some fraction of this period [13–16].

It is well known that the mean annual latitudes of sunspots vary by 12° – 15° over the 11-year cycle. Other spatial characteristics also change during the cycle. Consequently, distributions constructed over intervals of several (up to 11) years do not satisfy the

*E-mail:ivanov.vg@gao.spb.ru

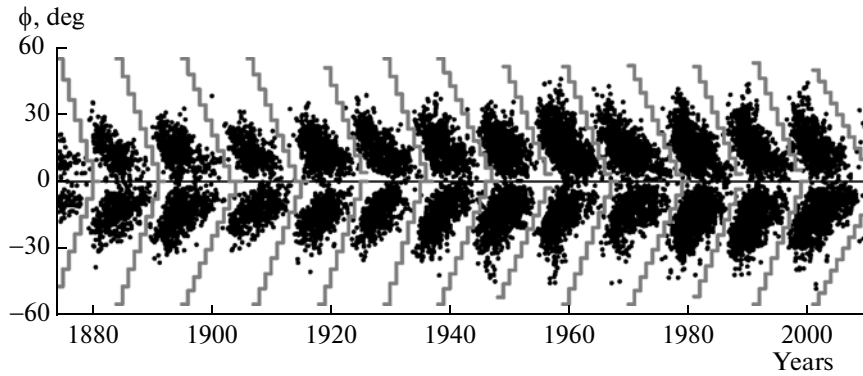


Fig. 1. The Maunder butterfly diagram. The grey broken lines indicate the boundary latitudes.

requirement that the statistical parameters of each sample studied be constant. Therefore, we chose an interval of one year as the basic time interval used to calculate the parameters of the latitude distributions, since the mean latitude varies only insignificantly over one year; at the same time, this interval ensures that the data samples are representative.

2. DATA SELECTION AND PROCESSING

For our study, we use the Greenwich Catalog of sunspot groups and its NOAA/USAF extension for 1874–2006.¹ Since the sunspots of different cycles must be considered separately, and these sunspots can coexist near the solar minima, we determined a boundary latitude for each year and each hemisphere, separating the upper sunspots of the new cycle (“upper wing”) from the lower sunspots of the old cycle (“lower wing”).

These sunspots can be separated in various ways. We used a simple technique based on separation in latitude (a similar technique is used, for example, in [4]). We selected the boundary latitudes dividing the wings based on the best correspondence to two conditions: (a) if the latitude distribution of the sunspots for a given year and a given hemisphere displays two maxima, the boundary latitude must be located between them; (b) the boundary latitudes for a selected pair of cycles decrease linearly with time. Thus, the boundary separating the wings is the set of broken lines formed by horizontal one-year segments (see Fig. 1). Our tests show that details of the boundary selection are almost insignificant for our study.

We describe the solar activity using the sunspot group index, whose daily value is defined as the number of groups observed on the disk on a given day. For the interval of the Greenwich Catalog, the mean

annual sunspot group indices G [3] are close to the corresponding GSN indices, to within a multiplicative factor [17, 18]. The indices G can be used to describe the solar activity of both the total disk and of a selected latitude interval, in particular, of an individual wing. For a given year and hemisphere, we have from two (if there is only one wing in each hemisphere) to four partial indices, whose sum equals the full index G . Since the latitude zones corresponding to the sunspots of the old and new cycles overlap with time, the curves of the partial indices can intersect each other near the solar minima (see Fig. 2).

Having selected a particular year and wing, we consider a subset of sunspot groups that is characterized by a mean heliographic latitude ϕ_0 and the density of the latitude distribution of sunspots $\rho(\phi)$. Thus, for a given year and wing, the number of sunspot groups n in the latitude interval $[\phi_1, \phi_2]$ is

$$n = G \int_{\phi_1}^{\phi_2} \rho(\phi - \phi_0) d\phi,$$

where G is the partial index of the number of sunspots for the selected wing, ϕ_0 is the mean latitude, and $\rho(\phi)$ is the relative (reduced to zero mean latitude) density of the latitude distribution of sunspots.

Let us first examine some mean features of the resulting annual distributions. For this purpose, we averaged the relative distributions of each hemisphere over all the observations and found the relative latitude distributions for the northern and southern hemispheres (see Fig. 3). For each distribution, we calculated the variance $\sigma^2 = \langle (\phi - \phi_0)^2 \rangle$ and two higher moments, namely, the skewness $\gamma_1 = \langle (\phi - \phi_0)^3 \rangle / \sigma^3$ and the kurtosis $\gamma_2 = \langle (\phi - \phi_0)^4 \rangle / \sigma^4 - 3$. These parameters are presented in the table. Note that in both hemispheres the distributions have similar forms that is close to the normal distribution.

¹<http://solarscience.msfc.nasa.gov/greenwch.shtml>

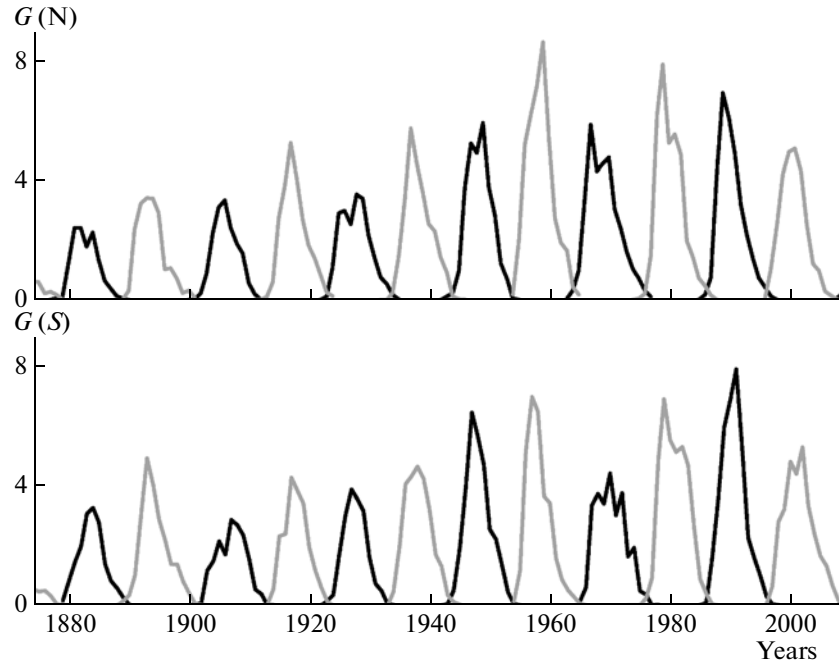


Fig. 2. Partial sunspot group indices for the northern, $G(N)$, and southern, $G(S)$, hemispheres. The black curves correspond to even solar cycles, and grey curves to odd cycles.

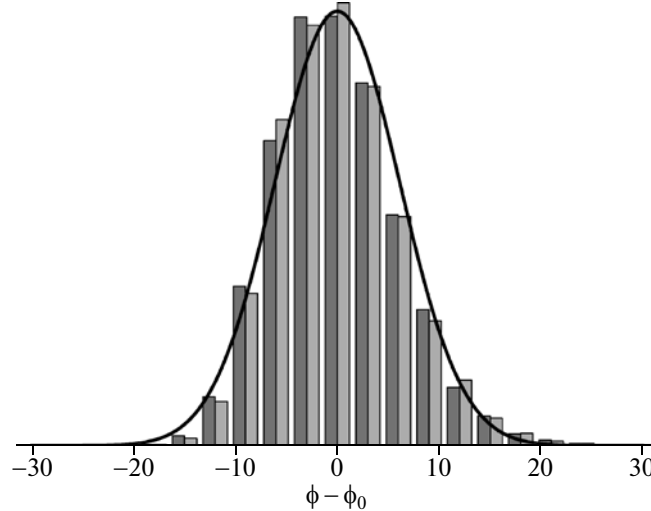


Fig. 3. Relative latitude distributions of sunspot groups for the northern (dark) and southern (light) hemispheres. The curve shows the normal distribution whose variance corresponds to the sunspots of the entire disk.

3. RELATIONS BETWEEN THE PARAMETERS OF THE SUNSPOT GROUP DISTRIBUTIONS AND THE ACTIVITY LEVEL

To examine the dependence of the sunspot distributions on the activity level, we divided all the annual latitude distributions into groups corresponding to partial indices G ranging from G_0 to $G_0 + 1$ for a given year and wing (where $G_0 = 0, \dots, 7$), and construct

the relative sunspot distribution for each range (see Fig. 4). The distributions for the various activity levels are approximately normal, with their deviations from normality tending to increase with increasing activity level.

We also calculated the statistical moments σ^2 , γ_1 , and γ_2 introduced above for each annual distribution. Figure 5 presents the dependence of these moments on the partial index G . The dependence is strongest for the variance σ^2 (the linear correlation coefficient

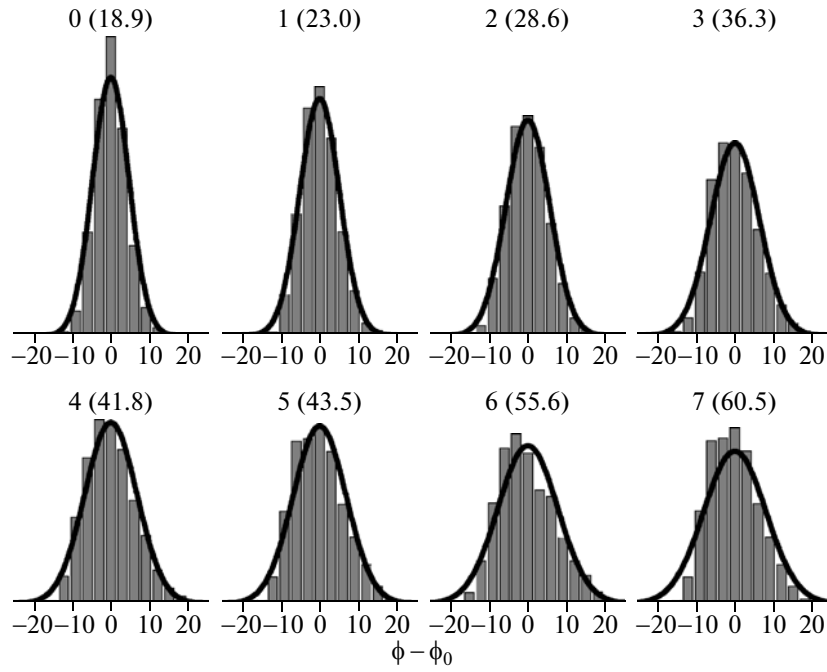


Fig. 4. Relative latitude distributions of sunspot groups for various activity levels $G_0 \leq G < G_0 + 1$. The numbers shown above the histograms indicate the lower limits G_0 of each activity range, while the numbers shown in parentheses correspond to the variance of the distribution σ_G^2 for each range (in square degrees). The curves correspond to normal distributions with the variance σ_G^2 .

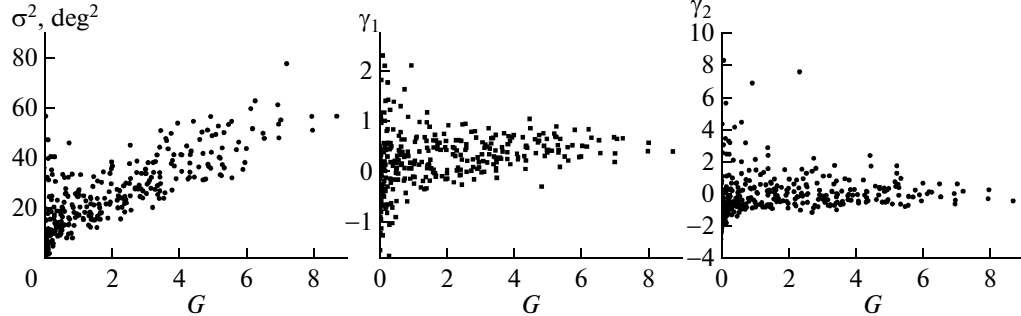


Fig. 5. Statistical moments of the annual latitude distributions σ^2 , γ_1 , and γ_2 as functions of the activity level G .

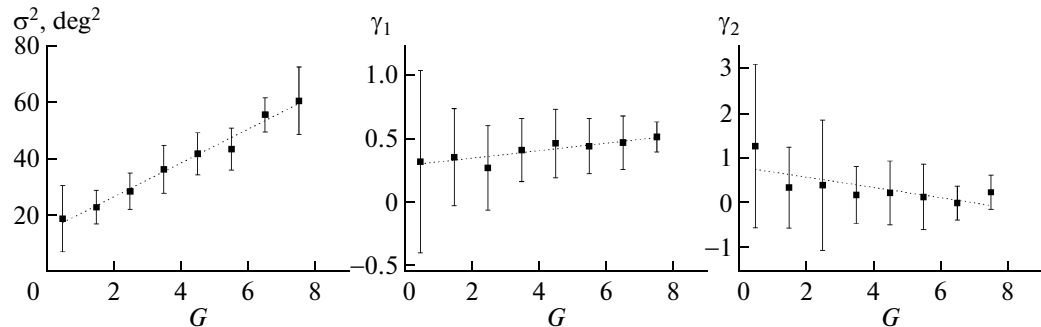


Fig. 6. Linear regression fits for the statistical moments of the annual latitude distributions σ^2 , γ_1 , and γ_2 as functions of the activity level G .

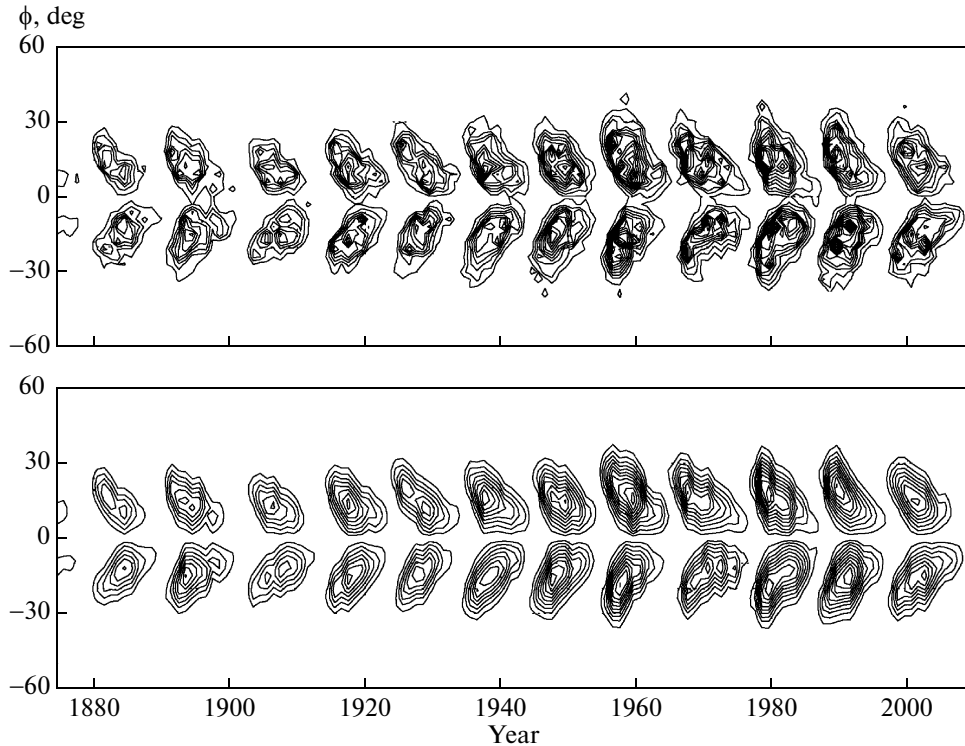


Fig. 7. Density distributions of the sunspot groups for the observed Maunder diagrams (top) and the “quasi-reconstructions” of these diagrams (bottom). The distance between the contours of equal density corresponds to a step of $0.0365 \text{ deg}^{-1} \text{ days}^{-1}$.

$r = 0.81$), in good agreement with our earlier conclusions [2]; the higher moments are almost independent of the activity level ($r = 0.28$ for γ_1 and $r = 0.11$ for γ_2).

Let us represent the results obtained in another form, by averaging the statistical moments of the sunspot distributions over each activity range $[G_0, G_0 + 1]$ used above. Figure 6 presents the linear regression fits obtained, with the vertical bars showing the rms deviations for each activity range.

The dependence of the variance on G is well described by the linear relation

$$\sigma^2(G) = (6.0 \pm 0.3)G + (14.5 \pm 1.5) \text{ deg}^2.$$

The relations between G and deviations from a normal distribution, γ_1 and γ_2 , are less pronounced. However, the asymmetry ratio γ_1 tends to increase and the excess γ_2 to decrease with increased activity. The corresponding linear regression fits take the forms

$$\gamma_1(G) = (0.030 \pm 0.007)G + (0.30 \pm 0.03)$$

and

$$\gamma_2(G) = -(0.11 \pm 0.04)G + (0.8 \pm 0.2).$$

The slight increase in the asymmetry results from the expansion of the sunspot zone to higher latitudes

with increasing activity, whereas this zone remains constrained by the equator from lower latitudes.

Thus, to first approximation, the latitude distributions obey normal laws with the density

$$\rho(\phi) = \frac{1}{\sqrt{2\pi\sigma^2(G)}} e^{-\frac{(\phi-\phi_0)^2}{2\sigma^2(G)}} \text{ deg}^{-1}, \quad (1)$$

where

$$\sigma^2(G) = 6.0G + 14.5 \text{ deg}^2. \quad (2)$$

To illustrate practical applications of (2), we used this dependence to make a mathematical model (“quasi-reconstruction”) of the Maunder butterfly diagram as follows. We assumed that the density of sunspot groups obeys (1), took the middle latitudes ϕ_0 from the observations, and calculated the variance σ^2 using (2) for the known activity levels G . The density

Parameters of the latitude distributions of sunspots in the N and S hemispheres

Hemisphere	ϕ_0 , deg	σ^2 , deg 2	γ_1	γ_2
N	15.0	37.9	0.21	-1.65
S	14.8	37.1	0.23	-1.67

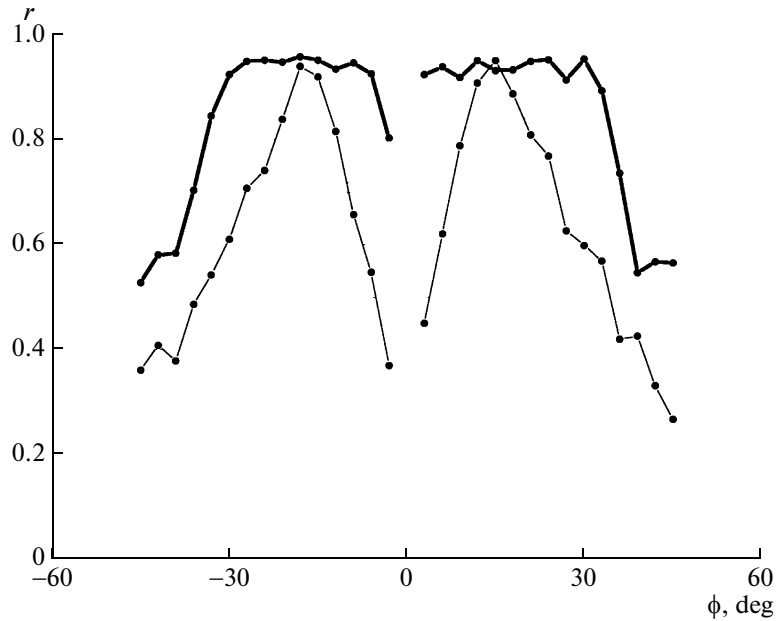


Fig. 8. Correlation $r(\phi)$ between the density of sunspot groups $\rho_{\text{obs}}(\phi, t)$ for the diagram observed at a given latitude ϕ and the corresponding $\rho_{\text{qr}}(\phi, t)$ for the “quasi-reconstruction” of the Maunder diagram (bold curve). The thin curve shows the correlation between $\rho_{\text{obs}}(\phi, t)$ and the number of sunspot groups in the selected hemisphere.

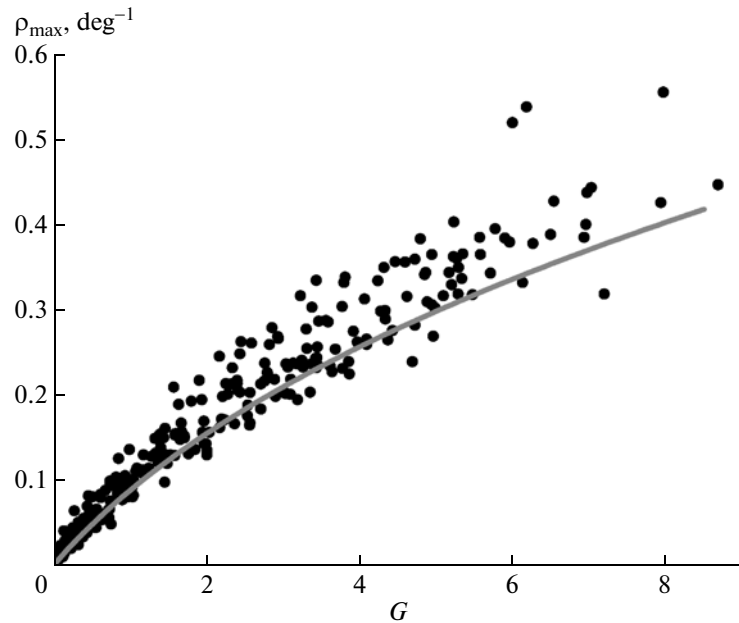


Fig. 9. Dependence of the latitude maxima of the sunspot density ρ_{max} on the activity level G satisfying the formula (3) (curve) and the observed dependence (points).

diagram obtained this way is shown at the bottom of Fig. 7, and the observed Maunder diagram is presented at its top. The observed diagram differs from the reconstructed one only in some small feature of the density distributions and a few rare events observed at the outer borders of the “butterfly wings,”

which are not described by the normal distribution. To analyze the similarity between the calculated and observed diagrams, we can extract the densities corresponding to given latitudes ϕ ($\rho_{\text{obs}}(\phi, t)$ and $\rho_{\text{qr}}(\phi, t)$) and determine the correlation between the time series obtained. Figure 8 presents the resulting correlation

coefficient as a function of latitude. Within latitudes $5^\circ \leq \phi \leq 30^\circ$, the reconstructed and observed densities agree well, and the correlation coefficient exceeds 0.9. It is interesting to compare this quantity with the correlation between $\rho_{\text{obs}}(\phi, t)$ and the index of sunspot groups for the given hemisphere G shown in the same plot. The latter is considerably lower for all latitudes, except for the center of the “royal zone” (12° – 18°), where the density behavior is the same as that of the sunspot group index.

The latitude density of sunspots $\rho(\phi)$ takes its maximum near the mean latitude of sunspots ϕ_0 and decreases with distance from this latitude. In the approximation used, the dependence of the latitude maximum of the sunspot density ρ_{max} on the activity level G directly follows from the distribution law (1) and (2) and takes the form

$$\rho_{\text{max}}(G) = \frac{G}{\sqrt{2\pi(6G + 14.5)}} \text{ deg}^{-1}. \quad (3)$$

Thus, the maximum sunspot density ρ_{max} is to grow more slowly than the sunspot index G with increasing sunspot activity, in good agreement with the observations (see Fig. 9).

4. CONCLUSIONS

To first approximation, the annual distribution of sunspot groups on latitude obeys the normal law, with the variance being a linear function of the activity level G . Thus, the latitude size of the spotted zone increases with increasing activity, in agreement with the results presented in [2, 3]. There are some small systematic deviations of the latitude distribution of the sunspots from the normal law: the distribution is somewhat broader than the normal distribution in periods of low activity, and the asymmetry of the distribution increases with increasing activity.

Both the characteristic width of the sunspot zone σ and the latitude maximum of the sunspot density ρ_{max} grow more slowly than the activity level G .

Finally, we note again that the behavior obtained can be used to impose constraints on models of the solar and stellar cyclicity. These laws can also be applied to reconstruct the spatial distribution of the activity over the solar disk in the past using the available activity levels.

ACKNOWLEDGMENTS

The authors thank V.N. Obridko for valuable remarks. This work was supported by the Russian Foundation for Basic Research (projects 09-02-00083, 10-02-00391, and 11-02-00755), the State Program of Support for Leading Scientific Schools of the Russian Federation (project code NSh-3645.2010.2), the program of the Presidium of the Russian Academy of Sciences “The Origin, Formation, and Evolution of Objects in the Universe,” and the Federal Targeted Program “The Scientific and Science-Education Staff of Innovative Russia.”

REFERENCES

1. W. Gleissberg, Z. Astrophys. **46**, 219 (1958).
2. E. V. Miletsky and V. G. Ivanov, Astron. Rep. **53**, 857 (2009).
3. V. G. Ivanov and E. V. Miletsky, Solar Phys. **268**, 231 (2011).
4. S. K. Solanki, T. Wenzler, and D. Schmitt, Astron. Astrophys. **483**, 623 (2008).
5. K. M. Kuzanyan and D. Sokoloff, Solar Phys. **173**, 1 (1997).
6. Yu. A. Nagovitsyn, V. G. Ivanov, E. V. Miletsky, and E. Yu. Nagovitsyna, Astron. Rep. **54**, 476 (2010).
7. I. G. Usoskin, D. Sokoloff, and D. Moss, Solar Phys. **254**, 345 (2009).
8. M. A. Livshits, I. Yu. Alekseev, and M. M. Katsova, Astron. Rep. **47**, 562 (2003).
9. M. M. Katsova, M. A. Livshits, and G. Belvedere, Solar Phys. **216**, 353 (2003).
10. A. Antalova and M. N. Gnevyshev, Contrib. Astron. Observ. Skalnat'e Pleso **11**, 63 (1983).
11. P. J. Pulkkinen, J. Brooke, J. Pelt, and I. Tuominen, Astron. Astrophys. **341**, L43 (1999).
12. K. J. Li, J. X. Wang, L. S. Zhan, et al., Solar Phys. **215**, 99 (2003).
13. Yu. I. Vitinsky, Soln. Dannye, No. 2, 107 (1989).
14. Yu. I. Vitinsky, Soln. Dannye, No. 8, 104 (1989).
15. Yu. I. Vitinsky, Soln. Dannye, No. 7, 97 (1990).
16. Yu. I. Vitinsky, Soln. Dannye, No. 8, 88 (1990).
17. D. V. Hoyt and K. H. Schatten, Solar Phys. **179**, 189 (1998).
18. D. V. Hoyt and K. H. Schatten, Solar Phys. **216**, 353 (1998).

Translated by V. Badin